J. Nucl. Phys. Mat. Sci. Rad. A. Vol. 6, No.1, Aug. 2018, pp.57–60

CHITKARA

Journal of Nuclear Physics, Material Sciences, Radiation and Applications
Journal homepage: https://jnp.chitkara.edu.in/

Improvements to the X-ray Spectrometer at the Aerosol Laboratory, Instituto de Física, UNAM

L V Mejía-Ponce, A E Hernández-López, S Reynoso-Cruces, J C Pineda, J A Mendoza-Flores, and J Miranda*

[1]*Institute of Physics, National Autonomous University of Mexico (UNAM), PO Box 20-364, 01000 Mexico City, Mexico*

*Email: miranda@fisica.unam.mx

ARTICLE INFORMATION

Received: June 14, 2018
Revised: July 06, 2018
Accepted: July 14, 2018

Published online: August 6, 2018

Keywords:
X-ray fluorescence analysis, Silicon Drift Detector SDD, chemical composition of atmospheric aerosols, Standard Reference Material 2783

DOI: 10.15415/jnp.2018.61009

ABSTRACT

Due to the demands of better (accurate and precise) analytical results using X-ray Fluorescence (XRF) at the Aerosol Laboratory, Instituto de Física, UNAM, it was necessary to carry out improvements in instrumentation and analytical procedures in the x-ray spectrometer located in this facility. A new turbomolecular vacuum system was installed, which allows reaching the working pressure in a shorter time. Characteristic x-rays are registered with a Silicon Drift Detector, or SDD, (8 mm thick Be window, 140 eV at 5.9 keV resolution), working directly in a high-vacuum, permitting the detection of x-rays with energies as low as 1 keV (Na Ka) and higher counting rates than in the past. Due to the interference produced by the Rh L x-rays emitted by the tube normally used for atmospheric and food analysis with Cl K x-rays, another tube with a W anode was mounted in the spectrometer to avoid this interference, with the possibility to select operation with any of these tubes. Examples of applications in atmospheric aerosols and other samples are presented, to demonstrate the enhanced function of the spectrometer. Other future modifications are also explained.

1. Introduction

The fast advance of science in certain fields requires frequently the knowledge of the chemical composition of samples. In particular, the determination of trace elements concentrations needs sensitive and non-destructive analytical methods, such as spectrometric techniques. These scientific disciplines include materials science, agriculture, art, medicine, biology, archaeology, geology, and environmental sciences [1]. Among the spectrometric techniques, those based on x-rays as the secondary radiation, are especially important [2]. The most common are X-Ray Fluorescence (XRF), Electron Probe Microanalysis (EPMA), Particle Induced X-ray Emission (PIXE), and Extended X-ray Absorption Fine Structure (EXAFS). Specifically, XRF can be based on the use of different primary radiation emitters (like radioactive sources, x-ray tubes, or synchrotron light). Recently, a multipurpose x-ray spectrometer was developed, mainly for the analysis of environmental samples [3]. It has been applied in several studies, focused on air pollution studies [4] and food chemistry [5]. In these works, several issues were identified, which limited the results obtained with the XRF analysis. Therefore, several improvements to the operation of the x-ray spectrometer were carried out, in order to be obtain more accurate, precise, and sensitive results with XRF. In the present work, the upgrades, aimed to detect lighter elements x-rays than before, eliminate peak interferences, and faster vacuum conditions, are detailed.

2. Materials and Methods

A complete description of the design and characterization of the spectrometer was given by Espinosa *et al.* [3], and the operation demonstrated the need to optimize its performance. The enhancements to the device referred to three main aspects: the obtention of better and faster high vacuum conditions in the irradiation chamber, detection of light elements, and reduction in the interference produced by the x-ray tube distinctive lines with the sample's characteristic x-rays. They are thoroughly described below.

2.1 Vacuum System

The original design of the spectrometer included a *Varian*® vacuum system, consisting of a 969-9369 turbomolecular pump, with a 130 L s^{-1} speed for N_2, supported by a SD-40 rotary vane pump (2.4 m^3 h^{-1} pumping speed). The system was substituted by a *Leybold*® package, integrated by a *Turbovac* 350 iX turbomolecular pump, showing a 290 L s^{-1} pumping speed for N_2, together with a *Trivac* D 8B rotary vane pump (10.2 m^3 h^{-1} pumping speed). The new system, moreover, is operated through a personal computer

ISSN No.: 2321-8649(Print) ISSN No.: 2321-9289(Online); Registration No. : CHAENG/2018/51628

interface, which allows an easier monitoring of the system. The test of the vacuum system was carried out by measuring the pressure inside the irradiation chamber with a *Digital DVM* series 6000-TC (MDV Vacuum) thermocouple gauge for low vacuum and a cold cathode gauge PDR series 900 (A&N Corporation) for high vacuum (down to 1.3×10^{-4} Pa). Thus, the time taken by the system to reach the working pressures was measured, both with the chamber empty and with a set of samples loaded inside the spectrometer.

2.2 Excitation Sources

The versatility of the spectrometer permits the installation of at least two primary radiation excitation sources at the same time, although preferably they do not operate simultaneously. Therefore, the improvement in this case was the mounting of two x-ray tubes with different anodes, Rh and W. Both of them are 75 W (maximum voltage 50 kV) packaged x-ray tubes, produced by Oxford Instruments X-Ray Technologies (Scotts Valley, CA, USA). The geometry of the system is sketched in Fig. 1. The Rh tube is set in such a way that its primary beam impinges normally on the surface of the sample, while the W tube is located at a 45° angle with respect to the sample's normal, on a horizontal plane. As the tubes have a 127 μm thick Be window at the exit, it is possible to work with them directly in a high vacuum. Both primary beams were reduced to 5 mm diameters with Pb collimators, with no filters at the exit. Therefore, the presence of Rh K and L lines is perceived in the primary spectrum, along with the W L and M x-rays when the respective tube is employed. Especially, the Rh L lines produce a strong interference with the Cl K lines, being an element of primary interest in many studies. On the other hand, the W M lines may produce an interference with the Si K lines. Thus, a complementary use of both tubes offers a good alternative to have more accurate analyses. To check the operation and influence of the tubes, the voltage was set at 50 kV and the current at 500 μA.

2.3 Detection System

The development of new technologies for x-ray detection, such as the *Silicon Drift Detector* (SDD), has an important impact on the spread of these spectrometries, especially XRF. This kind of detectors have small sizes, excellent resolutions and capabilities for processing high counting rates. Moreover, the cost has dropped substantially. Therefore, it was possible to adapt an SDD to the x-ray spectrometer. The device selected is an *Amptek® XSDD-123* complete spectrometer, which includes power source, amplifier, pulse processor and multichannel analyzer in a single module. The detector has an active area of 25 mm^2, a resolution of 140 eV at 5.9 keV, and an 8 μm thick Be window. A nylon adapter was designed to introduce the detector nose into the irradiation chamber, so it also operates under high vacuum. Additionally, an *Amptek®* Si-PIN *XR-100 CR* detector was placed in the same position as the SDD, as well as at a 45° angle above the Rh tube (position 2 in Fig. 1). Also, the Si-PIN in position 2 was evaluated with the inclusion of an Al filter in front of it, to eliminate low energy x-rays. The signal produced by the Si-PIN detector was processed by its own amplifier and the spectra collected by an *Ortec®* 926 multichannel analyzer. All the resulting x-ray spectra were analyzed by means of the *AXIL* computer code [6]. In this case, the performance of the detection systems was evaluated through the determination of sensitivity curves for each detector with a Rh x-ray tube (50 kV, 500 μA), using K and L x-ray lines. A set of Micromatter® (Vancouver, Canada) thin film standards was irradiated, separately for each tube. All the aforementioned upgrades, together, allowed to obtain better analytical outcomes using XRF on different types of samples, as will be described below.

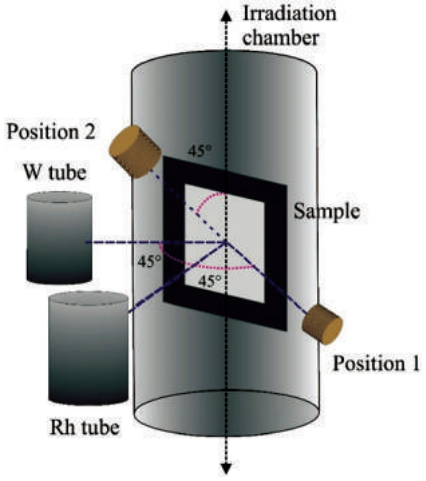

Figure 1. Diagram showing the geometric location of the x-ray tubes and detectors in the spectrometer. The SDD is located in position 1 and the Si-PIN in position 2.

3. Results and Discussion

The performance of the vacuum system is summarized in Figure 2. There, the pressure in the irradiation chamber is plotted as a function of the pumping time, with no samples and after the insertion of a sample set. It is apparent that there is virtually no difference between these two conditions. Moreover, a satisfactory operation pressure is reached in about 15 min after changing (inserting) the samples. The effect of the new vacuum system is observed also in the ultimate pressure attained in the chamber, as with the older system the 10^{-6} torr pressure range was never reached, even in the absence of samples. A comparison of the response $k(Z)$ of the detection systems, where Z is the atomic number of the target element, is observed in

Figure 3, which includes the SDD and the Si-PIN diode under the conditions described above. Here, the advantage of using the SDD under vacuum is evident, as the response is strongly increased for light elements (Na, Mg, Al, Si), in contrast with the Si-PIN in the same position. In particular, when $Z = 13$ (Al) $k(Z)$ is around two orders of magnitude higher for the SDD. An increase in $k(Z)$ is appreciated in the range $11 \leq Z \leq 16$, due to the presence of the Rh L lines in the primary spectrum, which have maximum photoelectric cross sections for those light elements. The placement of the Si-PIN detector in position 2 also reduces the values of $k(Z)$, because it presents a smaller solid angle than in position 1. Finally, the values determined for the Si-PIN diode with the Al filter clearly reflect the attenuation, although it does not strongly affect the response for higher energy x-rays, emitted by heavier elements ($Z > 30$ for K lines, $Z > 70$ in L lines).

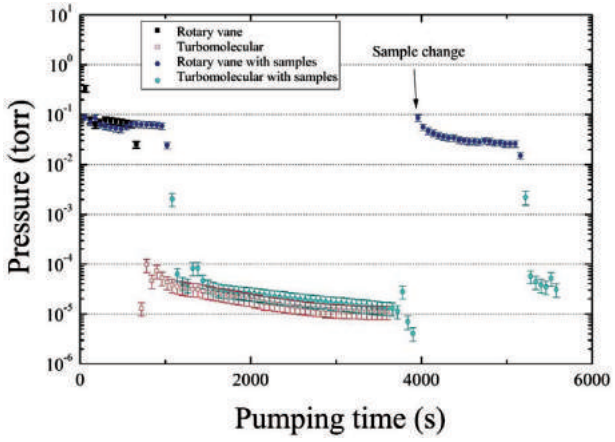

Figure 2. Pressure measured in the irradiation chamber as a function of the pumping time. The point where samples were changed inside the chamber is highlighted.

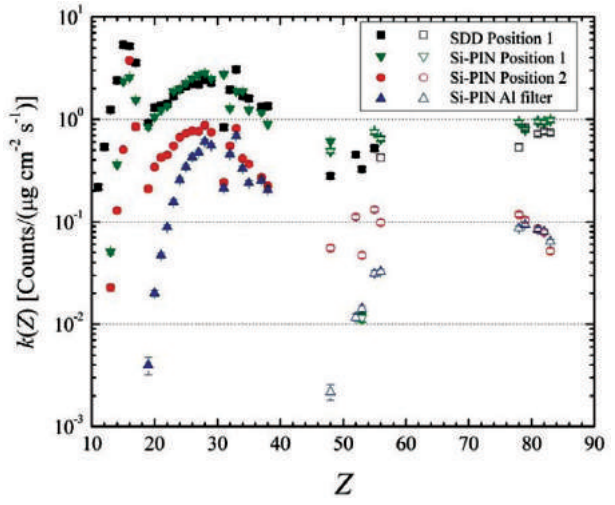

Figure 3. Response values $k(Z)$ as a function of the thin film standards atomic number Z, irradiated with a Rh x-ray tube (50 kV, 500 μA). Filled symbols correspond to K x-rays, while empty symbols correspond to L lines.

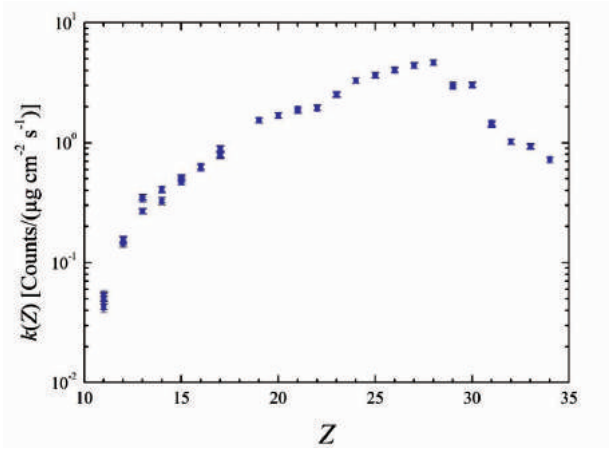

Figure 4. Response values $k(Z)$ as a function of the thin film standards atomic number Z, irradiated with a W x-ray tube (50 kV, 500 μA). The lines used were the K x-rays.

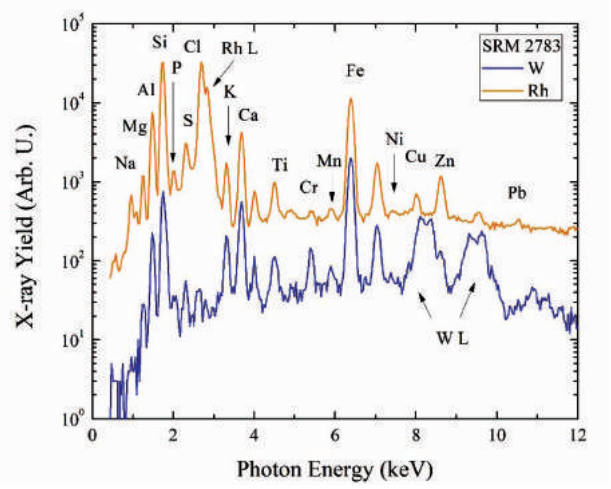

Figure 5. X-ray spectra from SRM 2783, irradiated with Rh and W tubes.

Regarding the use of the different x-ray tubes, an example of the response curves is displayed in Figure 4, where the $k(Z)$ values obtained with the W tube of are shown. Although it was expected, the response does not present a sharp increase for any element due to the W M lines, like the light elements irradiated by the Rh tube. The spectra acquired by irradiation of the NIST 2783 Standard Reference Material (SRM) with both tubes are displayed in Figure 5. It is possible to observe the interference of the Rh L lines with Cl K lines when the Rh tube is used, and the interference of the W L lines with the K lines of Cu and Zn. This justifies the use of both tubes for an accurate analysis. Moreover, the presence of intense Na, Mg and

Al peaks emphasize the advantage of using the SDD in vacuum. Additionally, the improved detector resolution allows a better identification of x-ray lines, reflected in a more accurate integration of the peak areas using AXIL. An estimation of the accuracy of the quantitative analyses obtained with the upgrades made to the x-ray spectrometer is seen in Table 1, presenting the results for the SRM 2783, where the certified and measured values are compared. From here, it is noticeable that for several elements the results are excellent, while for others there is a certain error, which must be corrected in future measurements. Finally, it is possible to mention that the improvements to the x-ray spectrometer have been also applied in the analysis of food [7].

Table 1. Mass of elements (μg) measured in standard reference material SRM 2783 and x-ray tube used in the measurements.

Element	Certified		Measured		Anode
Na	1860	(50)[a]	2559	(300)	W
Mg	8620	(260)	5866	(550)	W
Al	23210	(270)	24488	(1200)	W
Si	58600	(500)	49993	(2500)	Rh
S	1050	(130)	1888	(360)	W
Cl	ND		1219	(250)	W
K	5280	(260)	4334	(490)	W
Ca	13200	(850)	13985	(710)	Rh
Ti	1490	(120)	1920	(250)	Rh
V	48.5	(3)	66	(14)	Rh
Cr	135	(12)	145	(20)	Rh
Mn	320	(6)	300	(35)	Rh
Fe	26500	(800)	27419	(2400)	Rh
Ni	68	(6)	58	(21)	W
Cu	404	(21)	621	(58)	Rh
Zn	1790	(65)	2103	(190)	Rh
As	11.8	(1)	44	(10)	Rh
Cd	ND		303	(130)	W
Pb	317	(27)	302	(47)	Rh

[a]Numbers between parenthesis represent standard combined uncertainty.

4. Conclusions

The improvements carried out in the x-ray fluorescence spectrometer provide much better results, both from the accuracy and precision (uncertainty) points of view. The possibility to reach vacuum conditions in a shorter time also increased the operating productivity during routine analyses, which are important when a large number of samples must be irradiated. The use of different x-ray tubes prevents the interference with lines of important elements (Si, S, and Cl, for instance). Finally, the detection of light elements (Na, Mg, Al) with reasonable high efficiencies represents an important advance in the characterization of environmental and food samples.

Acknowledgements

Work supported in part by DGAPA-UNAM (PAPIIT IN102615) and CONACyT (grant 253051).

References

[1] Z. B. Alfassi, *Non-destructive Elemental Analysis*. Oxford: Blackwell Science, Ed. (2001).

[2] R. E. Van Grieken, A. A. Markowicz, *Handbook of X-ray Spectrometry.* New York: Marcel Dekker, Eds. (2002).

[3] A. A. Espinosa, *et al.*, *Instrumentation Science and Technology* **40(3)**, 603–617 (2012). https://doi.org/10.1080/10739149.2012.693560

[4] R. V. Díaz, J. López-Monroy, J. Miranda, A. A. Espinosa, *Nuclear Instruments and Methods in Physics Research Section B: Beam Interactions with Materials and Atoms*, **318(1)**, 135-138 (2014). https://doi.org/10.1016/j.nimb.2013.05.095

[5] Romero-Dávila, E. J. Miranda, J. C. Pineda, *AIP Conference Proceedings* **1671**, paper 020006 (2015).

[6] Manual for QXAS. Vienna: International Atomic Energy Agency (IAEA) (1995).

[7] M. C. Hernández, *et al.*, *Journal of Nuclear Physics, Material Sciences, Radiation and Applications,* **5(1)**, 25–34 (2017). https://doi.org/10.15415/jnp.2017.51003